# Entanglement Witnessing: Neural Network Optimization and Experimental Realization

Oscar Scholin*,†, Richard Zheng†, Alec Roberson†, and Theresa W. Lynn†

†Department of Physics, Harvey Mudd College, *Department of Physics, Pomona College

## Summary

Entanglement is a unique and central phenomenon of quantum mechanics. This persistent correlation between the properties of a pair of particles can be harnessed in algorithms both in secure communication, such as super dense coding, and in computation, e.g. Grover's search. The ability to quickly and accurately verify entanglement between particles, therefore, is key to the quantum information revolution. We verify entanglement by measuring particles in different bases and then calculating statistical correlations between measurements on the two particles. Riccardi et al. [1] define a set of 6 entanglement witnesses $\{W\}$, which are operators for which a negative expectation value verifies entanglement and all separable (i.e., non-entangled) states have a non-negative expectation value, and have direct application for photonics systems. Last year's team [5] defined 9 more witnesses $\{W'\}$, grouped into three "triplets" based on the local measurements they require. We extend this work by training a neural network to use measurements done for $\{W\}$ to predict which $W'$ triplet, and thus which next set of measurements, are most likely to witness entanglement. We also demonstrate our adaptive witnessing strategy using photon pairs entangled in polarization.

## Trained Neural Network to Choose Next Measurement

The statistics of 36 different measurements are sufficient to completely characterize a two-qubit state. Only 12 of these measurements are required to test for entanglement using $\{W\}$ (see Table 1). If $W$ values do not witness entanglement for a particular state, we turn to the group of nine entanglement witnesses $W'$ defined by last year's team [5]. These are grouped into sets of three additional measurements each called "triplets," denoted $W'_{t_X}$ for $X \in [1, 2, 3]$ where the subscript $t$ indicates the triplet and the triplets are group based on the distinct sets of additional local measurements they require. We optimize the entanglement verification process by using the measurements already done for $W$ to ask which additional measurements are most likely to give a negative witness value, so we can verify entanglement – if present – with the smallest number of measurements.

We report on three models (see Table 2): "Population," an analytical method by Eritas Yang [4], "NN2," the previous best-performing neural network by Becca Verghese and Laney Goldman [3], and "NN5," our current model.

| Witness Set | Polarization Pairs To Measure |
|---|---|
| $W_1, W_2, W_3, W_4, W_5, W_6$ | HH, HV, VH, VV, DD, DA, AD, AA, RR, RL, LR, LL |
| $W'_1, W'_2, W'_3$ ($W_{t_1}$) | + DR, DL, AR, AL, RD, RA, LD, LA |
| $W'_4, W'_5, W'_6$ ($W_{t_2}$) | + RH, RV, LH, LV, HR, HL, VR, VL |
| $W'_7, W'_8, W_9$ ($W_{t_3}$) | + DH, DV, AH, AV, HD, HA, VD, VA |

**Table 1:** Entanglement witnesses and the local measurements they require, represented as polarization pairs. See Figure 2 for a pictorial representation of these bases.

We trained NN5 on computationally generated random mixed 2-qubit states following the method outlined in [2], restricting our data set to those which satisfy $\min W \geq 0$ and $\min W'_{t_X} < 0$ (30.2% of randomly generated states).

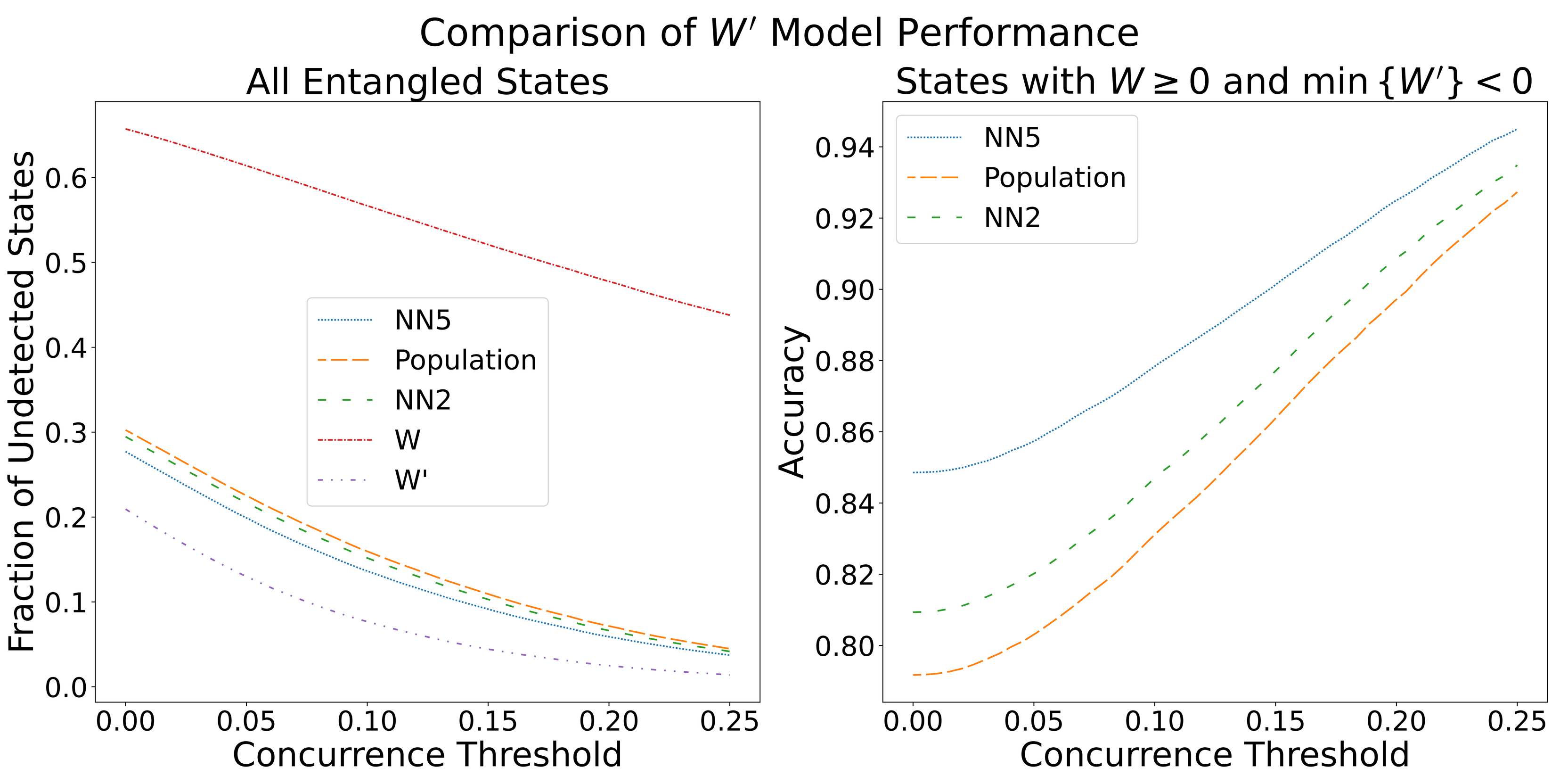


**Figure 1:** Performance comparison of adaptive models as a function of minimum entanglement (concurrence C, where C=1 is fully entangled). *(Left)*: fraction of all entangled states undetected by $\{W\}$ alone, plus a chosen $W'$ triplet, or plus all $\{W'\}$. *(Right)*: accuracy of adaptive choice (fraction of entangled states with $\min W \geq 0$ and $\min W'_{t_X} < 0$ that are successfully witnessed by the chosen $W'$ triplet).

| Model | Input Params | Architecture | UF, Acc |
|---|---|---|---|
| Pop. | $E_{HV}, E_{DA}, E_{RL}$ | Argmax of input | 30.3%, 79.2% |
| NN2 | HH, HV, VH, VV, DD, DA, AD, DD, RR, RL, LR, LL | 2 hidden layer NN | 29.5%, 80.9% |
| NN5 | HH, HV, VV, DD, DA, DD, RR, RL, LL | 5 hidden layer NN | 27.7%, 84.9% |

**Table 2:** Summary of model performance at concurrence threshold 0. UF is the undetected fraction of states on $2.7 \times 10^5$ unseen entangled states. Acc. is the accuracy when tested on a restricted $1.2 \times 10^5$ unseen states for which $\min W \geq 0$ and $\min W'_{t_X} < 0$. $XY$ is the probability of measuring $X$ state for the left and $Y$ for the right particle. Also, $E_{XY} = |0.5 - (XX + YY)|$. NN is neural network.

## Acknowledgements

We thank the following HMC funding sources: Physics Summer Research Fund (AR), Vandiver and Class of 69 Summer Research Funds (OS), Sprague Experiential Learning Program (RZ).

## Experimentally Demonstrated Performance

A schematic of our experimental quantum optics setup is shown in Figure 2. A pair of barium-borate (BBO) crystals perform Type I spontaneous parametric down-conversion (SPDC) to create entangled photons. We investigated the class of states $|E_0(\eta, \chi)\rangle = \cos\eta|\Psi^+\rangle + \sin\eta\, e^{i\chi}|\Psi^-\rangle$, where $|\Psi^\pm\rangle = \frac{1}{\sqrt{2}}\Big(|HV\rangle \pm |VH\rangle\Big)$. We test $E_0$ states with $\eta = 30°, 45°$ and $\chi$ swept from 0 to 90°. All these states are entangled with the exception of $|E_0(\eta = 45°, \chi = 0)\rangle$.

These states are interesting because their entanglement is not always detectable by $\{W\}$ but is by $\{W'\}$, which we verify experimentally. We determine $\min\{W\}$ and $\min\{W'_{t_1}, W'_{t_2}, W'_{t_3}\}$ by performing the correlated measurements in the necessary local polarization bases. The results, including a comparison to theory and purity-adjusted theory, are shown in Figure 3. For entangled states states $|E_0(\eta = 45°, \chi > 0)\rangle$ which are theoretically not witnessed by $\{W\}$, all three adaptive choice methods (NN5, NN2, and the population method) correctly predict the optimal set of next measurements based on the first round of data collected.

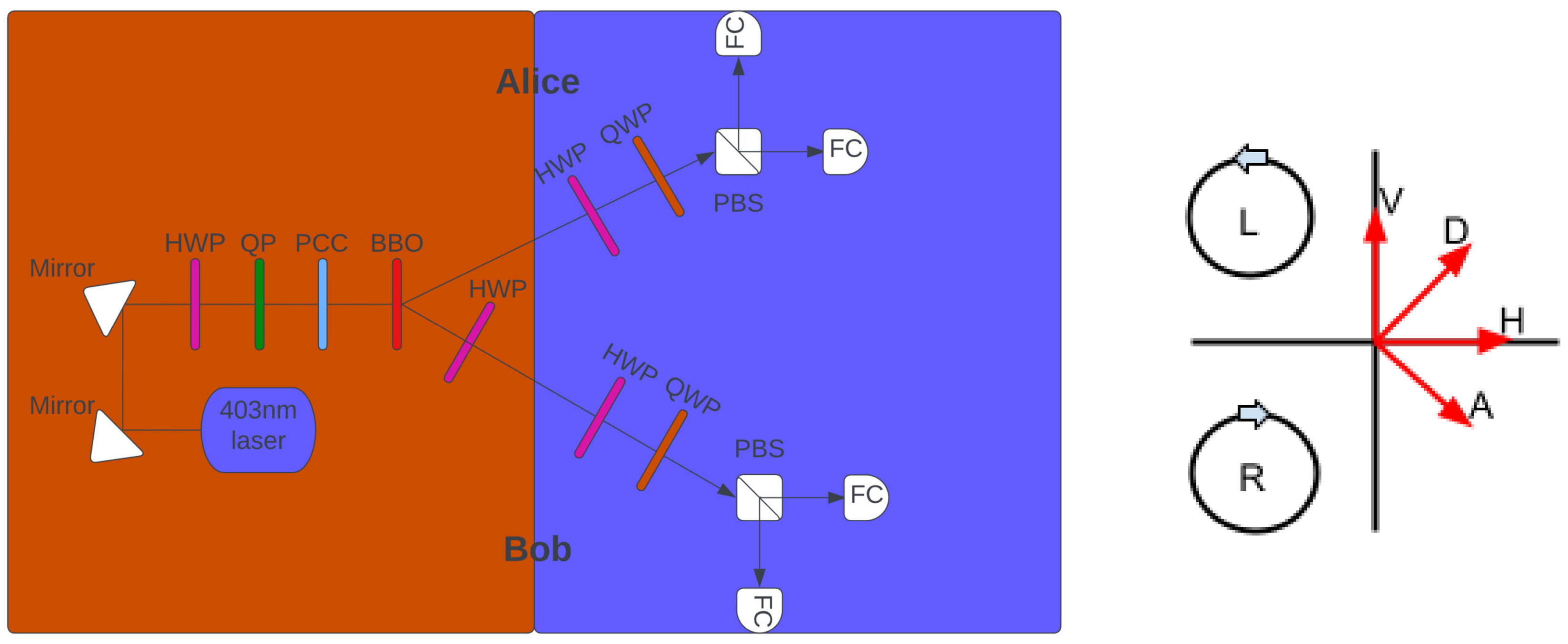


**Figure 2:** *(Left)* Experimental setup. The portion dedicated to the creation of states is highlighted in orange. We configure our measurement basis in the blue portion. HWP is half waveplate, QWP quarter waveplate, QP quartz plate, and PCC precompensation crystal. *(Right)* Representation of the different single particle polarization basis states.

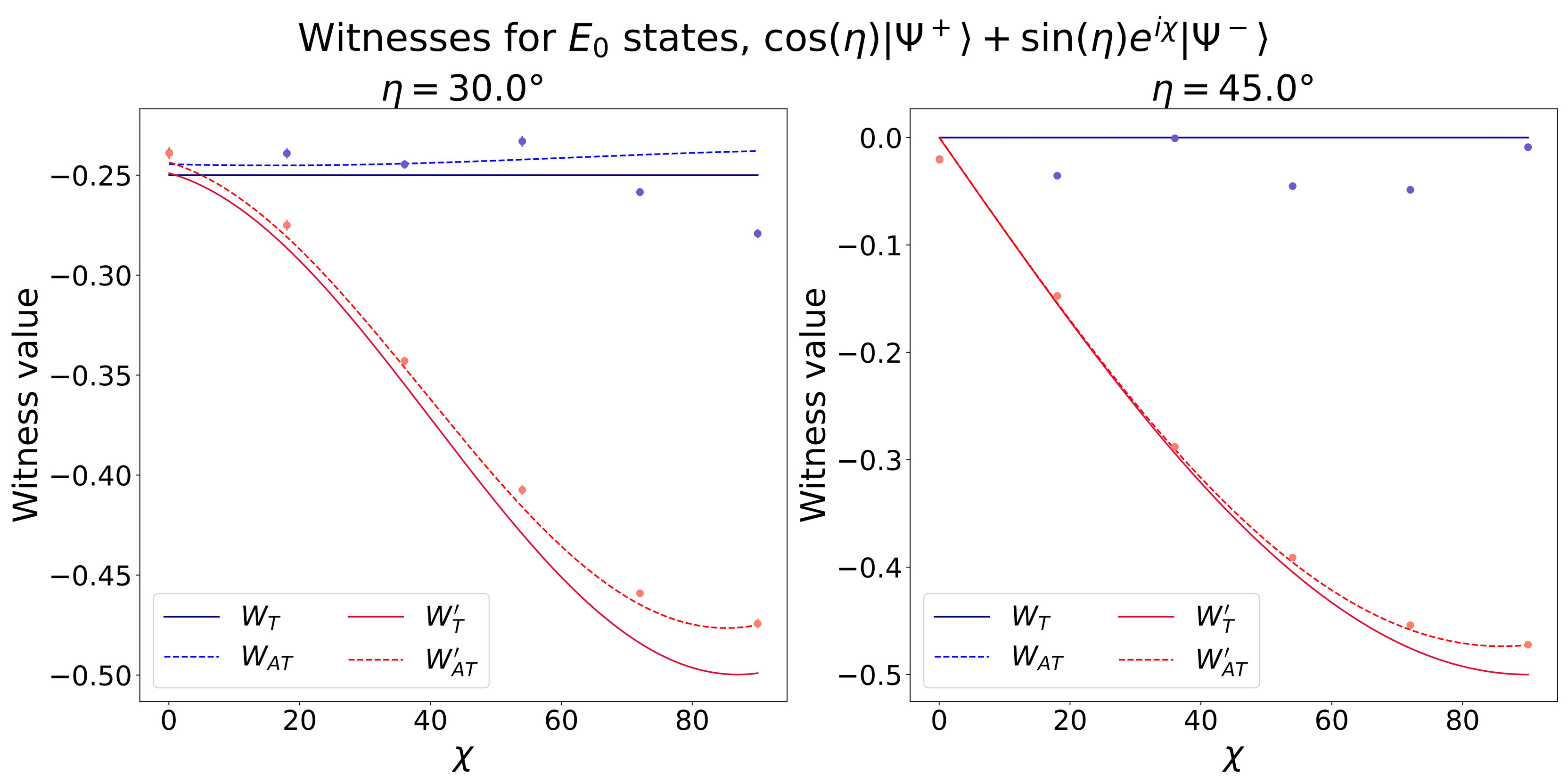


**Figure 3:** Experimentally measured $W$ (blue points) and $W'_{min}$ (red points). Error bars are included but too small to be seen. Also plotted for comparison are the theoretical and purity-adjusted theoretical values.

## References

[1] Alberto Riccardi, Dariusz Chruściński, and Chiara Macchiavello. "Optimal entanglement witnesses from limited local measurements". en. In: Physical Review A 101.6 (June 2020), p. 062319. ISSN: 2469-9926, 2469-9934. DOI: 10.1103/PhysRevA.101.062319. URL: https://link.aps.org/doi/10.1103/PhysRevA.101.062319 (visited on 05/24/2023).

[2] Jan Roik et al. "Accuracy of Entanglement Detection via Artificial Neural Networks and Human-Designed Entanglement Witnesses". In: Physical Review Applied 15.5 (May 2021). Publisher: American Physical Society, p. 054006. DOI: 10.1103/PhysRevApplied.15.054006. URL: https://link.aps.org/doi/10.1103/PhysRevApplied.15.054006 (visited on 05/30/2023).

[3] Becca Verghese and Laney Goldman. "Developing a Neural Network for Predicting W'". In: Unpublished (May 2023). URL: https://github.com/Lynn-Quantum-Optics/Summer-Spring-2022-3/blob/main/Summer2022/Spring_2023_Recap%20-Becca%20and%20Laney.pdf.

[4] Eritas Yang. "The population method". In: Unpublished (May 2023). URL: https://github.com/Lynn-Quantum-Optics/Summer-Spring-2022-3/blob/main/Summer2022/Spring_2023_Recap%20-%20Eritas.pdf.

[5] Eritas Yang, Becca Verghese, and Ben Hartley. "Entanglement Witness Writeup". In: Unpublished (July 2022). URL: https://github.com/Lynn-Quantum-Optics/Summer-Spring-2022-3/blob/main/Summer2022/summer-2022-QO_write_up.pdf.